DOI: 10.1002/cbic.200900192

Combinatorial Strategies by Marine Cyanobacteria: Symplostatin 4, an Antimitotic Natural Dolastatin 10/15 Hybrid that Synergizes with the Coproduced HDAC Inhibitor Largazole

Kanchan Taori,[a] Yanxia Liu,[a] Valerie J. Paul,[b] and Hendrik Luesch*[a]

Dolastatins 10 and 15 are potent cytotoxic agents,[1] derivatives of which, named TZT-1027 (auristatin PE) and cematodin/synthadotin, respectively, are in phase II cancer clinical trials.[2] Major structural differences between dolastatin 10 and dolastatin 15 include the C-terminal residues and the presence of modified internal amino acid residues through the apparent incorporation of acetate units in dolastatin 10; this is presumably produced by the alternating action of polyketide synthases and nonribosomal peptide synthetases (Figure 1). Whereas the dolastatins were originally isolated from the sea hare *Dolabella auricularia*, overwhelming circumstantial evidence has been accumulated that the dolastatins are actually produced by cyanobacteria and then sequestered through diet.[3] In particular, dolastatin 10[4] and the closely related compounds symplostatin 1,[5] symplostatin 3,[6] and malevamide D[7] were isolated from cyanobacteria of the genus *Symploca*, as was belamide A,[8] which may be considered a truncated dolastatin 15 analogue with an internal deletion. Unnatural target molecules that contain features of both dolastatins 10 and 15 have been made synthetically with the goal of generating new diversity around these scaffolds and gaining insight into the structure–activity relationship (SAR) for these mitotic inhibitors by using synthetic organic chemistry.[9] Here we report the isolation, structure determination, biological activity, and mechanism of action of a dolastatin 10/15 hybrid, symplostatin 4 (**1**),[10] which has the same planar structure as the recently reported antimalarial compound gallinamide A (Figure 1).[11,12] Motifs from both the dolastatin 10 and dolastatin 15 structures reappear in the structure of compound **1** (Figure 1). Intriguingly, the same cyanobacterium also produces largazole,[13] which exerts a fundamentally different mode of action through inhibition of histone deacetylases (HDACs).[14] We tested the hypothesis that both molecules might be coproduced to exert cooperative effects on target cells; this can be exploited for anticancer combination therapy.

A sample of the marine cyanobacterium *Symploca* sp. was collected from Key Largo (Florida Keys) and extracted with organic solvents. Cytotoxicity-guided fractionation included solvent partitioning, normal-phase chromatography, and then reversed-phase HPLC; this yielded largazole, the more potent cytotoxin, and symplostatin 4 (**1**), the only other cytotoxic agent in this extract, as a colorless, amorphous solid.

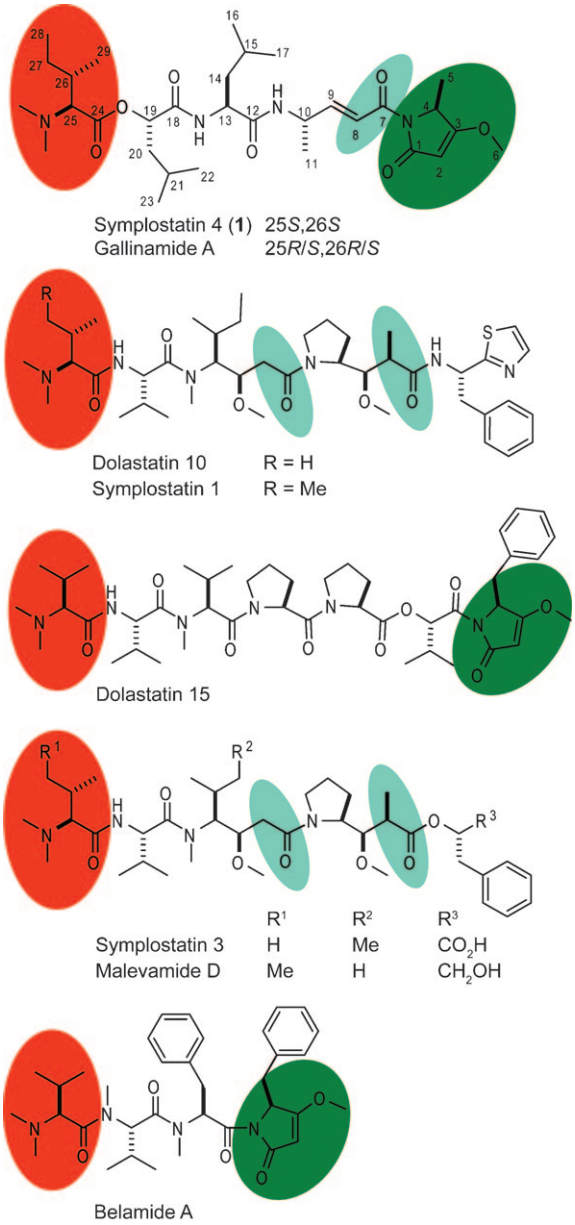

Figure 1. Structures of dolastatin 10, its cyanobacterial analogues symplostatins 1 and 3 and malevamide D, as well as dolastatin 15, its truncated analogue belamide A and the hybrid-like symplostatin 4 (**1**) and gallinamide A. All compounds except dolastatin 15 have been isolated from cyanobacteria. Characteristic features for each compound are indicated.

[a] *K. Taori, Dr. Y. Liu, Prof. Dr. H. Luesch*
Department of Medicinal Chemistry, University of Florida
1600 SW Archer Road, Gainesville, Florida 32610 (USA)
Fax: (+1) 352-273-7741
E-mail: luesch@cop.ufl.edu

[b] *Dr. V. J. Paul*
Smithsonian Marine Station
701 Seaway Drive, Fort Pierce, Florida 34949 (USA)

Supporting information for this article is available on the WWW under http://dx.doi.org/10.1002/cbic.200900192.

The molecular formula of **1** was determined to be $C_{31}H_{52}N_4O_7$ by HR-ESI/APCI-MS ($[M+H]^+$, *m/z* 593.3921). A detailed analysis of ^{1}H NMR, ^{13}C NMR, COSY, HSQC and HMBC spectroscopic data in $CDCl_3$ (Table 1) revealed that **1** is a depsipeptide consisting of leucine, 2-hydroxyisocaproic acid, 4-amino-pent-2*E*-enoic acid, *N*,*N*-dimethyl isoleucine, and a substituted pyrrolinone. Sequencing of the three most C-terminal units was readily achieved by using HMBC spectroscopy. At the N terminus, the 2-hydroxyisocaproic acid unit was connected as shown by NOESY correlations between the NH of leucine and the α-proton (H19) of the hydroxy acid. By default the hydroxy acid had to be linked through an ester bond to the terminal *N*,*N*-dimethyl isoleucine unit; this established the structure as depicted for **1**. The NMR spectroscopy-derived sequence was confirmed by tandem ESI mass spectrometry (Figure 2).

Table 1. NMR spectroscopy data for symplostatin 4 (**1**) in $CDCl_3$ at 600 MHz (^{1}H) and 150 MHz (^{13}C).

C/H no.	δ_H (*J* in Hz)	δ_C, mult.	HMBC[a]
1	–	169.7, qC	–
2	5.03, s	93.0, CH	1,4
3	–	180.7, qC	–
4	4.59, q (6.5)	55.7, CH	1, 2, 3, 5, 7
5	1.48, d (6.5)	17.1, CH_3	3, 4
6	3.86, s	58.7, CH_3	3
7	–	164.2, qC	–
8	7.39, d (15.6)	122.4, CH	7, 9, 10
9	6.96, dd (15.6, 5.0)	148.2, CH	7, 8, 10, 11
10	4.70, m	46.2, CH	8, 9, 11, 12
11	1.30, d (6.9)	19.9, CH_3	9, 10
10-NH	6.37, d (5.7)	–	–
12	–	171.0, qC	–
13	4.45, br dd (7.8, 7.8)	52.0, CH	12, 14, 15
14a	1.67, m	40.9, CH_2	15, 16, 17
14b	1.62, m	–	15, 16, 17
15	1.66, m	24.7, CH	–
16	0.95, d[b]	22.91,[c] CH_3	14, 15
17	0.93, d (6.3)	21.5, CH_3	14, 15
13-NH	7.14, br s	–	–
18	–	169.4,[d,e] qC	–
19	5.19, dd (9.3, 4.2)	74.7,[d] CH	18, 20, 21
20a	1.82, m	40.8, CH_2	18, 23
20b	1.63, m	–	18, 21, 23
21	1.65, m	24.5, CH	18
22	0.94, d[b]	22.89,[c] CH_3	20, 21
23	0.91, br d (5)	21.8, CH_3	20, 21
24	–	174.7,[e] qC	–
25	3.57, br s	72.0, CH	–
26	1.99, br m	33.8, CH	–
27a	1.63, m	26.1,[d] CH_2	25, 28, 29
27b	1.31, m	–	–
28	0.96, t[b]	11.1,[d] CH_3	26, 27
29	1.03, br d (5.3)	15.1,[d] CH_3	–
30a/b	2.79, br s (6H)	41.7,[d] CH_3 ×2	–

[a] Protons showing HMBC correlations to the indicated carbon. [b] *J* not deduced due to signal overlap. [c] Interchangeable. [d] Broad signal. [e] Tentative assignment (signal in the ^{13}C NMR spectrum without HMBC).

The absolute configuration of **1** was determined by chiral HPLC analysis and comparison of retention times with authentic standards. Acid hydrolysis (6 N HCl, 110 °C, 24 h) liberated L-leucine, *N*,*N*-dimethyl-L-isoleucine, and (*S*)-2-hydroxyisocaproic acid. To determine the absolute configuration at C4 and C10 we carried out ozonolysis followed by oxidative work-up and acid hydrolysis as above to liberate two equivalents of alanine. One intense additional peak for L-alanine and lack of a peak for D-alanine in the chromatographic profile of the acid hydrolyzate compared with the previous profile indicated that the configuration in **1** was 4*S*,10*S*.

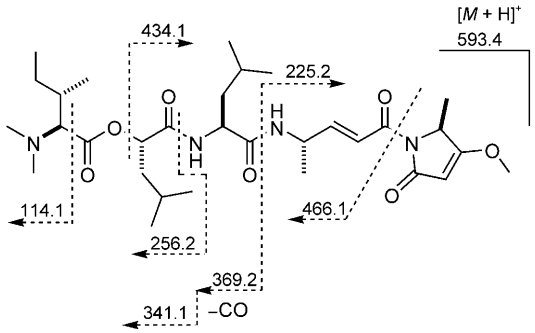

Figure 2. Fragmentation pattern of symplostatin 4 (**1**) by ESI-MS/MS.

Compound **1** was assayed for cancer cell growth inhibitory activity against two human cancer cell lines. It was moderately active against HeLa cervical carcinoma cells and slightly less active against HT-29 colon adenocarcinoma with IC_{50} values of 12 and 53 μM, respectively. Symplostatin 4 (**1**) shares structural features of both the potent cytotoxins dolastatins 10 and 15, including an *N*,*N*-dimethyl amino acid residue on the N terminus, which is present in both dolastatins, a substituted pyrrolinone on the C terminus similar to the one in dolastatin 15, and a dehydrated statine-like unit through acetate incorporation into the backbone as in dolastatin 10 (Figure 1). This structural resemblance to dolastatins 10 and 15 prompted us to investigate whether the cellular effects of **1** and dolastatins 10 and 15 are similar. Because dolastatins 10 and 15 are potent disruptors of microtubule polymers[15] we examined the effects of symplostatin 4 (**1**) on cellular microtubules by indirect immunofluorescence in A-10 embryonic rat smooth-muscle cells, the cytoskeleton of which is easy to visualize.[16] Even though A-10 cells were relatively insensitive to the effects of symplostatin 4 (**1**), starting at 50 μM the cellular microtubules network appeared clearly disrupted (Figure 3). Complete microtubule depolymerization was not achieved even at 100 μM. For comparison, the dolastatin 10 homologue symplostatin 1 (*N*,*N*-Me_2-Ile instead of *N*,*N*-Me_2-Val) showed similar effects already at 1 nM (data not shown), in agreement with published data.[16] Because microtubule disruption is expected to prevent the formation of a functional mitotic spindle and consequently mitosis we carried out DNA content analysis by flow cytometry. Exposure of HT-29 cells to symplostatin 4 (**1**) resulted in a pronounced accumulation of cells harboring 4N content of chromosomes after 18 h (Figure 4), indeed indicating cell cycle arrest in the G2/M phase due to prevention of mitosis as anticipated. However, this effect was again less severe than ob-

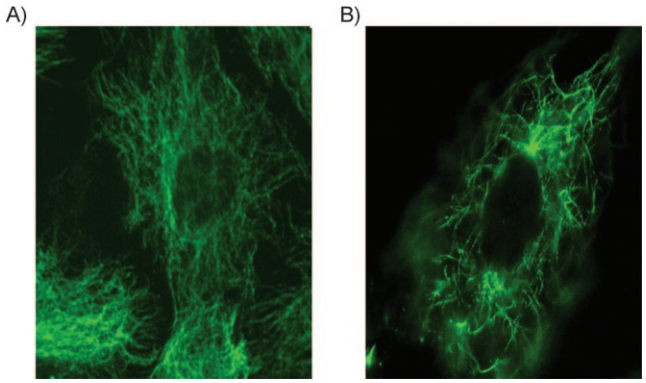

Figure 3. Effects of symplostatin 4 (**1**) on microtubules. A-10 cells were treated with A) vehicle (EtOH) or B) symplostatin 4 (50 μM) for 18 h and microtubules were visualized by indirect immunofluorescence with a monoclonal anti-β-tubulin antibody.

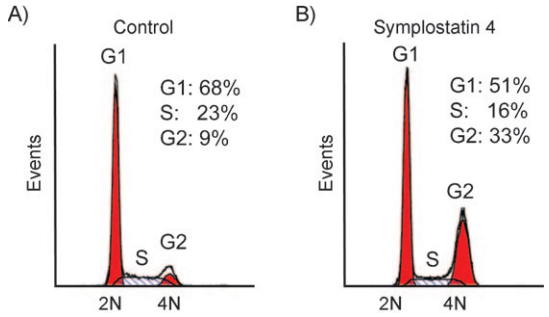

Figure 4. Effect of symplostatin 4 (**1**) on the cell cycle distribution. HT-29 cells were treated with A) vehicle (EtOH) or B) symplostatin 4 (50 μM) for 18 h, then fixed, stained with propidium iodide and analyzed by flow cytometry.

served for symplostatin 1[16] and secondary modes of action cannot be excluded.

Symplostatin 4 (**1**) is several magnitudes less potent than dolastatins 10 and 15 in all of the performed assays (cancer cell viability, effects on microtubules and cell cycle arrest) yet consistently causes similar phenotypes. The reduced potency can be attributed to several structural features (or lack thereof),[17] particularly in the three most N-terminal units.[18] First, the additional methylene group in the N-terminal unit is expected to slightly reduce activity because it is known that the N-terminal residue is critical for activity and that substitution of *N*,*N*-dimethyl valine with *N*,*N*-dimethyl isoleucine as in symplostatin 1 has resulted in only little loss of activity.[4,16] Second, the valine unit in dolastatins 10 and 15 is crucial for potent activity, and this residue is replaced by 2-hydroxyisocaproic acid with a more labile ester linkage, which would also affect the relative conformational freedom around that bond compared to the amide bond. Third, while the isobutyl sidechain in **1** compared with isopropyl in dolastatin 15 and *sec*-butyl in dolastatin 10 might not be a major reason for reduced activity, the lack of N-methylation at that position in **1** compared with dolastatins 10 and 15 might play a role. However, it has been reported that the corresponding N-demethyl analogue (dolaisoleuine unit) of dolastatin 10 showed equal in vivo antitumor activity against P388 leukemia in mice.[19] One more characteristic feature of **1** compared with dolastatin 10 is the nature of the acetate-derived unit, which formally corresponds to an elimination product of a statine-like unit. Such hybridization change from sp^3 to sp^2 in the corresponding dolaproine unit of dolastatin 10 resulted in a ~30-fold reduction in cytotoxicity and approximately fourfold reduction of the inhibitory effect on tubulin polymerization.[18b] Thus, we expect that this modification might also have contributed to reduced activities in our assays. Nevertheless, symplostatin 4 (**1**) retained moderate activity.

An intriguing fact is that the symplostatin-4-producing *Symploca* sp. also produced another structurally and mechanistically distinct cytotoxin, largazole, which prevents cancer cell growth through another epigenetic mechanism involving the inhibition of histone deacetylases (HDACs) upon metabolic activation by thioester hydrolysis.[13,14] Interestingly, HDAC inhibitors and tubulin agents such as paclitaxel (which stabilizes polymerized microtubules) show promise for combination therapy.[20] A synergistic response with paclitaxel has been reported for trichostatin A and suberoylanilide hydroxamic acid (SAHA), two HDAC inhibitors that do not discriminate well between enzyme isoforms. Cooperativity has been proposed to be due to inhibition of HDAC6,[20a] the enzyme that deacetylates α-tubulin; however, largazole shows selectivity for class I over class IIb enzyme HDAC6.[14] We tested the effect of simultaneous treatment of HT-29 cells with symplostatin 4 (**1**) and largazole at concentrations that would be largely ineffective if administered as single agents (~IC_{10}). The combination of both compounds was synergistic in reducing cancer cell viability (Figure 5A and B). Cell viability was reduced to 67±3%, which is less than the effect expected for an additive (zero interaction) response of the single agents (Loewe additivity)[21] of 72±2% ($p=0.05$, Figure 5B). With respect to cell growth, cotreatment resulted in 54±4% cell growth, which is less than the calculated additive (zero interaction) value of 60±2% ($p=0.05$, Figure 5C). The mechanism of synergy is likely different than for the combination of paclitaxel and SAHA,[20a] because largazole is not a potent HDAC6 inhibitor.[14] However, there is evidence that HDAC inhibitors also increase the chemosensitivity of cancer cells to anticancer drugs that act by other mechanisms.[22]

Chimeric structures derived from dolastatins 10 and 15 have been synthesized previously that retained potent cytotoxicity and activity against tubulin polymerization.[9] The structure of symplostatin 4 (**1**) and other dolastatin 10 or 15 analogues from *Symploca* spp. illustrates that these cyanobacteria have the potential to execute combinatorial biosynthesis; however, to date two or more dolastatin 10- and 15-related compounds have not yet been reported from the same collection or strain, perhaps because there would be no competitive advantage to the cyanobacterium. In contrast, other cyanobacteria such as *Nostoc* spp. have yielded numerous secondary metabolites with repeating motifs from the same strain.[23] In addition to being structural analogues of each other, the *Anabaena* metabolites called laxaphycins exert unusual biological synergism.[24]

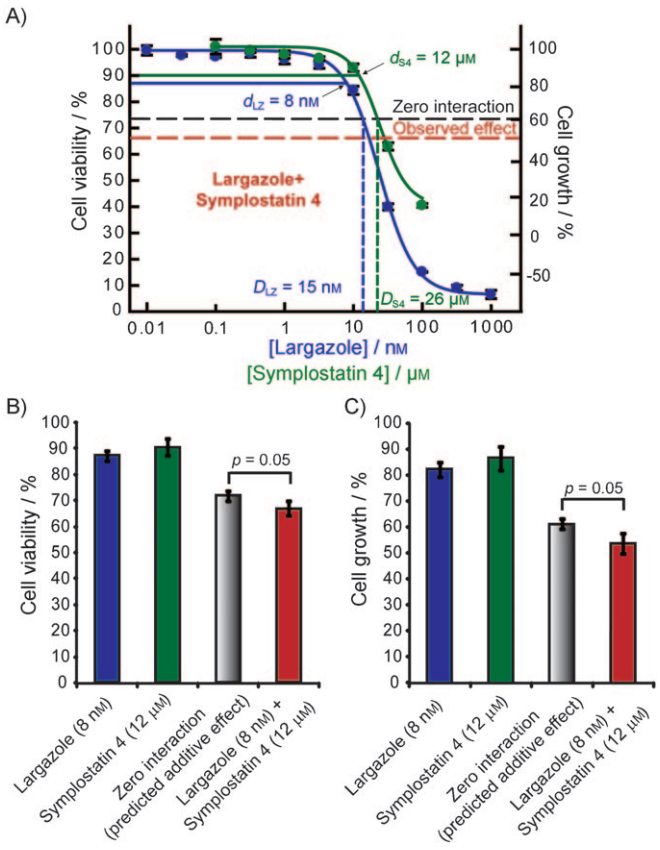

Figure 5. Cooperative effects of symplostatin 4 (S4) and largazole (LZ) on HT-29 cell viability and growth. A) Dose-response curves from duplicate measurements were recorded for single agents and the fitted equations established. An iterative approach was used to find the inhibition that satisfied the Loewe additivity combination index equation for two agents (x, y): $(d_x/D_x)+(d_y/D_y)=1$ (zero interaction), in which d_x and d_y are the concentrations of the two agents used in combination and D_x and D_y are isoeffective concentrations of the two agents.[21] B) Cell viability and C) cell growth upon treatment with individual agents (largazole, blue; symplostatin 4, green) and in combination (red). Error bars indicate standard deviation ($n=4$). For the expected response (zero interaction; gray), mean and standard deviation were calculated from the duplicate dose–response curve pairs ($n=4$), which each yielded a zero interaction value. Statistical significance was assessed by *t*-test ($p=0.05$).

There is an urgent need not only to discover new chemotherapeutic agents, but also to fully exploit the potential of existing drugs, for example through combination therapy. However, there has often been a lack of rationale in the selection of coadministered agents. Recent genomic approaches are proving useful to make more educated choices.[25] HDAC inhibitors appear particularly promising as adjunct therapy.[26] Our data demonstrate that cyanobacteria have evolved cooperative strategies by coproducing chemical defense agents that sensitize cells to the respective other agent. However, obviously intended target organisms differ from our experimental cellular systems. It is widely recognized that natural products play an essential role in drug discovery,[27] and particularly the microbial diversity in the ocean is an emerging vast resource for future drugs.[28] Here, marine cyanobacteria additionally demonstrate that they can guide us to design effective "rational" drug cocktails by employing "biomimetic" treatment strategies. Combinatorial biosynthesis meets combinatorial pharmacology in cyanobacteria. Further exploration of both concepts, cyanobacterial style, is warranted.

Experimental Section

General experimental procedures: ^{1}H, ^{13}C and 2D NMR spectroscopy data were recorded on a Bruker Avance II 600 MHz spectrometer equipped with a 1 mm triple resonance high-temperature superconducting cryogenic probe by using residual solvent signals (δ_H 7.26, δ_C 77.0 ppm) as internal standards. The HSQC experiments were optimized for $^1J_{CH}=145$ Hz, and the HMBC experiment for $^nJ_{CH}=7$ Hz. LC–MS/MS data were obtained by using an Agilent 1100 equipped with a ThermoFinnigan LCQ by ESI (positive mode). HRMS data was obtained by using an Agilent LC-TOF mass spectrometer equipped with an ESI/APCI multimode ion source detector (UCR Mass Spectrometry Facility, Department of Chemistry, University of California at Riverside). Authentic standards of alanine, leucine, and 2-hydroxyisocaproic acid isomers for chiral analysis were obtained from Sigma and *N*,*N*-dimethyl isoleucines synthesized as described.[29]

Extraction and isolation: A sample of *Symploca* sp. was collected from Pillars, Key Largo (Florida Keys, USA) in August 2003, freeze-dried, extracted with MeOH/EtOAc (1:1), and fractionated as described previously.[13] Briefly, the resulting lipophilic extract (0.29 g) was partitioned between hexanes and 80% aq MeOH. The aq MeOH layer was concentrated and fractionated by silica gel chromatography by using CH_2Cl_2 containing increasing amounts of *i*PrOH followed by MeOH. The fraction that eluted with 5% *i*PrOH was then subjected to reversed-phase HPLC (YMC-pack ODS-AQ, 250×10 mm, 2.0 mL min^{-1}; UV detection at 220 and 254 nm) by using a MeOH/H_2O linear gradient (40–100% for 75 min and then 100% MeOH for 10 min). Compound **1** eluted at t_R 57.5 min (0.6 mg) and largazole at t_R 61.5 min (1.2 mg).

Symplostatin 4 (1): colorless, amorphous powder; $[\alpha]_D^{20}=-53$ ($c=0.06$, MeOH); ^{1}H NMR, ^{13}C NMR and HMBC data, see Table 1; IR (film) $\nu_{max}=2919$, 2850, 1726, 1690, 1676, 1658, 1628, 1180, 1153, 1132, 1031, 890 cm^{-1}; UV (MeOH) λ_{max} (log ε): 210 (3.81), 250 (3.69); HR-ESI/APCI-MS *m/z* calcd for $C_{31}H_{53}N_4O_7$: 593.3914 $[M+H]^+$, found: 593.3921.

Determination of absolute configuration: A sample of compound **1** (50 μg) was suspended in 6 N HCl (0.5 mL) and heated at 110 °C for 24 h. The hydrolyzate was concentrated to dryness and subjected to chiral HPLC analysis. Amino acids were analyzed by using column 1 (Phenomenex Chirex phase 3126, *N*,*S*-dioctyl-D-penicillamine, 4.60×250 mm, 5 μm; solvent, 2 mM $CuSO_4$ in 95:5 H_2O/MeCN; flow rate, 0.75 mL min^{-1}; detection at 254 nm). The retention times (t_R, min) for standard amino acids were as follows: L-Me_2-Ile (17.4), D-Me_2-Ile (18.0), L-*allo*-Me_2-Ile (19.0), D-*allo*-Me_2Ile (19.9), L-Leu (53.2), D-Leu (66.2). Components in the hydrolyzate eluted at t_R 17.4 min (L-Me_2-Ile) and 53.2 min (L-Leu). Hydroxy acids were analyzed on column 2 (Chiral Technologies, Chiralpak WH, 4.60×250 mm, 5 μm; solvent, 2 mM $CuSO_4$; flow rate 0.75 mL min^{-1}; detection at 254 nm). The retention times (t_R, min) for the standards were as follows: (*S*)-(−)-2-hydroxyisocaproic acid (17.3), (*R*)-(+)-2-hydroxyisocaproic acid (20.8). 2-Hydroxyisocaproic acid in the hydrolyzate eluted at t_R 17.3 min, indicating the *S* configuration. To assign the other two stereocenters a sample of compound **1** (50 μg) was dissolved in CH_2Cl_2 (4 mL) and subjected to ozonolysis at room temperature for 30 min. The solvent was evaporated, and the residue was treated with H_2O_2/HCO_2H (1:2,

0.6 mL) at 70 °C for 20 min. The solvent was evaporated, and the resulting oxidation product was hydrolyzed with 6 N HCl (0.5 mL) at 110 °C for 24 h. The hydrolysis product was concentrated to dryness and analyzed by chiral HPLC by using column 1. When compared to the profile without prior ozonolysis, the HPLC profile showed one intense new peak for L-Ala (t_R 8.5 min) but no peak corresponding to D-Ala (t_R 10.2 min).

Cell culture: Cells were purchased from ATCC, culture medium from Invitrogen, and fetal bovine serum (FBS) from HyClone (Logan, UT, USA). Cells were propagated and maintained in DMEM medium (high glucose) that was supplemented with 10% FBS at 37 °C humidified air and 5% CO_2.

Cell viability assay: HT-29 and HeLa cells were plated in 96-well format and incubated at 37 °C (5% CO_2) for 24 h and then incubated with single compounds or binary compound mixtures (1% EtOH). After 48 h of incubation the cell viability was quantified by using an MTT-based assay kit according to the manufacturer's instructions (Promega). Antiproliferative effects were assessed as follows: $100 \times T/C =$ % cell viability, and $100 \times (T-T_0)/(C-T_0) =$ % cell growth [T = absorbance in treated wells (48 h); T_0 = absorbance at time zero; C = absorbance in control wells (48 h)]. Dose–response curve fitting was done by using Xlfit Excel, MathIQ version 2.2.2 (IDBS Ltd.). Additive values were calculated based on Loewe additivity (see Figure 5).[21]

Indirect immunofluorescence: A-10 cells (1×10^5 cells per coverslip) were grown on glass coverslips for 24 h, then treated with symplostatin 4, vehicle control (EtOH), or positive control (symplostatin 1) and incubated for 18 h. Cells were then fixed with MeOH (−20 °C, 10 min), blocked for 20 min (10% sheep serum in 0.1% Tris-buffered saline with Tween (TBST)), and incubated for 2 h with monoclonal anti-β-tubulin antibody (T-4026, Sigma). Following a series of washes, the cells were incubated with FITC-conjugated sheep anti-mouse IgG (F-3008, Sigma) for 1 h. The coverslips were washed, the nuclear material was stained with 4′,6-diamidino-2-phenylindole (DAPI, 15 μg mL^{-1}) and examined and photographed by using a Zeiss Upright Microscope.

Cell cycle analysis: To investigate the effect of symplostatin 4 on cell cycle progression, HT-29 cells were treated with 50 μM symplostatin 4 or vehicle control for 18 h. The cells were fixed with 70% EtOH (−20 °C, 30 min), the RNA digested with RNase A and DNA stained with propidium iodide. The DNA content was analyzed by using a FACS Calibur System (BD Biosciences, San Jose, CA).

Acknowledgements

Financial support was provided by the Florida Sea Grant College Program with support from NOAA, Office of Sea Grant, U.S. Department of Commerce (Grant No. NA06OAR4170014) and the University of Florida College of Pharmacy. We acknowledge NSF for funding through the External User Program of the National High Magnetic Field Laboratory (NHMFL), which supported our NMR studies at the Advanced Magnetic Resonance Imaging and Spectroscopy (AMRIS) facility in the McKnight Brain Institute of the University of Florida (UF). The 600 MHz 1 mm triple-resonance HTS cryogenic probe was developed through collaboration between UF, NHMFL, and Bruker Biospin. We thank M. Becerro for extracting the cyanobacterium, J. Rocca for assistance in NMR data acquisition, S. McClellan for flow cytometry, Dr. J. Johnson for the MS/MS analysis and Professors W. H. Gerwick and R. G. Linington for providing NMR spectra of gallinamide A in $CDCl_3$. This is contribution 779 from the Smithsonian Marine Station at Fort Pierce.

Keywords: dolastatins · marine cyanobacteria · natural products · structure elucidation · structure–activity relationships

[1] a) G. R. Pettit, Y. Kamano, C. L. Herald, A. A. Tuinman, F. E. Boettner, H. Kizu, J. M. Schmidt, L. Baczynskyi, K. B. Tomer, R. J. Bontems, *J. Am. Chem. Soc.* **1987**, *109*, 6883–6885; b) G. R. Pettit, Y. Kamano, C. Dufresne, R. L. Cerny, C. L. Herald, J. M. Schmidt, *J. Org. Chem.* **1989**, *54*, 6005–6006.

[2] a) D. J. Newman, G. M. Cragg, *J. Nat. Prod.* **2004**, *67*, 1216–1238; b) T. L. Simmons, E. Andrianasolo, K. McPhail, P. Flatt, W. H. Gerwick, *Mol. Cancer Ther.* **2005**, *4*, 333–342.

[3] H. Luesch, G. G. Harrigan, G. Goetz, F. D. Horgen, *Curr. Med. Chem.* **2002**, *9*, 1791–1806.

[4] H. Luesch, R. E. Moore, V. J. Paul, S. L. Mooberry, T. H. Corbett, *J. Nat. Prod.* **2001**, *64*, 907–910.

[5] G. G. Harrigan, H. Luesch, W. Y. Yoshida, R. E. Moore, D. G. Nagle, V. J. Paul, S. L. Mooberry, T. H. Corbett, F. A. Valeriote, *J. Nat. Prod.* **1998**, *61*, 1075–1077.

[6] H. Luesch, W. Y. Yoshida, R. E. Moore, V. J. Paul, S. L. Mooberry, T. H. Corbett, *J. Nat. Prod.* **2002**, *65*, 16–20.

[7] F. D. Horgen, E. B. Kazmierski, H. E. Westenburg, W. Y. Yoshida, P. J. Scheuer, *J. Nat. Prod.* **2002**, *65*, 487–491.

[8] T. L. Simmons, K. L. McPhail, E. Ortega-Barría, S. L. Mooberry, W. H. Gerwick, *Tetrahedron Lett.* **2006**, *47*, 3387–3390.

[9] J. Poncet, M. Busquet, F. Roux, A. Pierré, G. Atassi, P. Jouin, *J. Med. Chem.* **1998**, *41*, 1524–1530.

[10] The structure and activity of symplostatin 4 (**1**) was presented at the Masters defense by K. T. (Gainesville, Florida, May 29, 2008) and by H. L. at The 22nd Naito Conference on Chemical Biology [I] (Sapporo, Japan, September 12, 2008).

[11] R. G. Linington, B. R. Clark, E. E. Trimble, A. Almanza, L.-D. Ureña, D. E. Kyle, W. H. Gerwick, *J. Nat. Prod.* **2009**, *72*, 14–17.

[12] The absolute configuration of the N-terminal residue of gallinamide A was not determined. Comparison of ^{1}H and ^{13}C NMR spectra in $CDCl_3$ for **1** and for gallinamide A (provided by Professors Gerwick and Linington) showed dissimilarity for the N-terminal region, suggesting that the compounds might not be identical.

[13] K. Taori, V. J. Paul, H. Luesch, *J. Am. Chem. Soc.* **2008**, *130*, 1806–1807.

[14] Y. Ying, K. Taori, H. Kim, J. Hong, H. Luesch, *J. Am. Chem. Soc.* **2008**, *130*, 8455–8459.

[15] E. Hamel, *Biopolymers* **2002**, *66*, 142–160.

[16] S. L. Mooberry, R. M. Leal, T. L. Tinley, H. Luesch, R. E. Moore, T. H. Corbett, *Int. J. Cancer* **2003**, *104*, 512–521.

[17] a) G. R. Pettit, J. K. Srirangam, J. Barkoczy, M. D. Williams, M. R. Boyd, E. Hamel, R. K. Pettit, F. Hogan, R. Bai, J.-C. Chapuis, S. C. McAllister, J. M. Schmidt, *Anti-Cancer Drug Des.* **1998**, *13*, 243–277; b) E. Hamel, D. G. Covell, *Curr. Med. Chem.-Anti-Cancer Agents* **2002**, *2*, 19–53; and references therein.

[18] a) R. Bai, G. R. Pettit, E. Hamel, *Biochem. Pharmacol.* **1990**, *40*, 1859–1864; b) R. Bai, M. C. Roach, S. K. Jayaram, J. Barkoczy, G. R. Pettit, R. F. Ludeña, E. Hamel, *Biochem. Pharmacol.* **1993**, *45*, 1503–1515; c) A. Mitra, D. Sept, *Biochemistry* **2004**, *43*, 13955–13962.

[19] K. Miyazaki, M. Kobayashi, T. Natsume, M. Gondo, T. Mikami, K. Sakakibara, S. Tsukagoshi, *Chem. Pharm. Bull.* **1995**, *43*, 1706–1718.

[20] a) S. C. Dowdy, S. Jiang, X. C. Zhou, X. Hou, F. Jin, K. C. Podratz, S.-W. Jiang, *Mol. Cancer Ther.* **2006**, *5*, 2767–2776; b) A. L. Cooper, V. L. Greenberg, P. S. Lancaster, J. R. van Nagell Jr. , S. G. Zimmer, S. C. Modescitt, *Gynecol. Oncol.* **2007**, *104*, 596–601.

[21] M. C. Berenbaum, *Pharmacol. Rev.* **1989**, *41*, 93–141.

[22] X. Zhang, M. Yashiro, J. Ren, K. Hirakawa, *Oncol. Rep.* **2006**, *16*, 563–568.

[23] a) C. Mehner, D. Müller, S. Kehraus, S. Hautmann, M. Gütschow, G. M. König, *ChemBioChem* **2008**, *9*, 2692–2703; b) T. Golakoti, J. Ogino, T. L.

Husebo, C. M. Jensen, L. K. Larsen, G. M. L. Patterson, R. E. Moore, S. L. Mooberry, T. H. Corbett, F. A. Valeriote, *J. Am. Chem. Soc.* **1995**, *117*, 12030–12049.
[24] a) W. P. Frankmölle, L. K. Larsen, F. R. Caplan, G. M. Patterson, G. Knübel, I. A. Levine, R. E. Moore, *J. Antibiot.* **1992**, *45*, 1451–1457; b) I. Bonnard, M. Rolland, J.-M. Salmon, E. Debiton, C. Barthomeuf, B. Banaigs, *J. Med. Chem.* **2007**, *50*, 1266–1279.
[25] a) S. R. Bartz, Z. Zhang, J. Burchard, M. Imakura, M. Martin, A. Palmieri, R. Needham, J. Guo, M. Gordon, N. Chung, P. Warrener, A. L. Jackson, M. Carleton, M. Oatley, L. Locco, F. Santini, T. Smith, P. Kunapuli, M. Ferrer, B. Strulovici, S. H. Friend, P. S. Linsley, *Mol. Cell. Biol.* **2006**, *26*, 9377–9386; b) A. W. Whitehurst, B. O. Bodemann, J. Cardenas, D. Ferguson, L. Girard, M. Peyton, J. D. Minna, C. Michnoff, W. Hao, M. G. Roth, X.-J. Xie, M. A. White, *Nature* **2007**, *446*, 815–819.
[26] J. S. Carew, F. J. Giles, S. T. Nawrocki, *Cancer Lett.* **2008**, *269*, 7–17.
[27] D. J. Newman, G. M. Cragg, *J. Nat. Prod.* **2007**, *70*, 461–477.
[28] W. Fenical, P. R. Jensen, *Nat. Chem. Biol.* **2006**, *2*, 666–673.
[29] R. E. Bowman, H. H. Stroud, *J. Chem. Soc.* **1950**, 1342–1345.

Received: March 30, 2009
Published online on June 9, 2009

